Submitted to ApJL, May 21 2004
Preprint typeset using LaTeX style emulateapj v. 4/12/04

arXiv:astro-ph/0405436 v1 21 May 2004

AN X-RAY JET FROM A WHITE DWARF – DETECTION OF THE COLLIMATED OUTFLOW FROM CH CYGNI WITH *CHANDRA*

Duncan K. Galloway
Center for Space Research, 37-626b, Massachusetts Institute of Technology, Cambridge, MA 02139

and

J. L. Sokoloski*
Smithsonian Astrophysical Observatory, 60 Garden St., Cambridge, MA 02138

Submitted to ApJL, May 21 2004

ABSTRACT

Most symbiotic stars consist of a white dwarf accreting material from the wind of a red giant. A growing number of these objects have been found to produce jets. Analysis of archival *Chandra* data of the symbiotic system CH Cygni reveals faint extended emission to the south, aligned with the optical and radio jets seen in earlier *HST* and VLA observations. CH Cygni thus contains only the second known white dwarf with an X-ray jet, after R Aquarii.

Subject headings: binaries: symbiotic — stars: individual (CH Cygni) — stars: winds, outflows — white dwarfs — X-rays: general

1. INTRODUCTION

Collimated jets are produced by many astrophysical systems, ranging from proto-stars, through stellar-mass black holes in X-ray binaries, to active galactic nuclei. Jets are intimately related to the process of accretion. The angular momentum of the accreting material typically leads to the formation of a disk, and observationally, many systems with disks also produce jets. Symbiotic stars, in which a white dwarf (WD) accretes from the wind of a red giant, are probably the most recently recognized class of jet-producing objects. There are currently at least 10-12 symbiotics with evidence for bipolar outflows (Brocksopp et al. 2004; Corradi et al. 2001). Very little is known about the X-ray properties of symbiotic-star jets, as only one symbiotic jet has been reported in the X-rays (R Aquarii; see Kellogg et al. 2001).

CH Cygni ($l = 81.^\circ86$, $b = +15.^\circ58$) is one of the best-studied symbiotic binaries. The system consists of a white dwarf accreting from a red giant companion, and surrounded by an ionized emission-line nebula (for a review of CH Cyg's properties see Kenyon 2001). The multiple photometric and radial velocity periodicities present in the system suggest the presence of a third star (Hinkle et al. 1993). Estimates of the distance are 100–300 pc (e.g. Kenyon 1986; Ivison et al. 1991; Munari et al. 1996; Viotti et al. 1997). We adopt 245 ± 50 pc, from the mode of the Hipparcos parallax probability distribution (Perryman et al. 1997). A radio jet was first detected between April 1984 and May 1985, coincident with a strong radio outburst and a substantial decline in the visual magnitude (Taylor et al. 1986). Subsequent observations in the radio and optical wavebands revealed that the jet position angle on the sky changes with time, suggesting that the jet axis precesses with a period of $\approx$ 6520 d (Crocker et al. 2002). Changes in the fast optical flickering in 1997, after a jet was produced, have also suggested a direct connection between the accretion disk and jet production in CH Cyg (Sokoloski & Kenyon 2003a). X-ray emission was first conclusively detected from the system by *EXOSAT* on 1985 May 24, at a flux of $\sim 1.3 \times 10^{-11}$ ergs cm^{-2} s^{-1} (0.02–2.5 keV; Leahy & Taylor 1987). Subsequent *ASCA* observations revealed a complex X-ray spectrum which could be fit either with multiple thermal components (Ezuka et al. 1998) or a single-temperature thermal spectrum attenuated by an ionized absorber (Wheatley 2001).

Here we describe analysis of a *Chandra* observation in which we detect, for the first time, the X-ray jet in CH Cyg.

2. OBSERVATIONS

We analyzed a 47 ks observation of CH Cyg acquired between 2001 March 27 06:22 and 20:02 UT, by the *Chandra X-ray Observatory* (Weisskopf et al. 2002). The observation of CH Cyg was made in FAINT mode with the high-energy transmission grating (HETG) in place, although the source flux was too low to obtain a high signal-to-noise grating spectrum (the first-order count rate was 6.3×10^{-3} count s^{-1}). Thus, we did not consider the dispersed spectra for our analysis. The CCDs are sensitive to photons in the 0.2–10 keV energy range, and have a pixel size of $0.''492$. The zeroth-order image fell on the S3 (backside-illuminated) chip of the ACIS-S array. The observation was performed in timed mode, for which the CCDs are read out every 3.24 s. The standard data filtering resulted in a net exposure time of 47.082 ks. To analyze these archival data, we used CIAO[1] software version 3.0.2 and the *Chandra* calibration database version 2.26.

3. RESULTS

CH Cyg was detected with a total zeroth order count rate of 1.95×10^{-2} count s^{-1}. The image was not affected by pile-up. The centroid position was R.A. $= 19^{\rm h}24^{\rm m}33.^{\rm s}076$, decl. $= +50^\circ14'29.''21$ (J2000.0),

Electronic address: duncan@space.mit.edu
*NSF Astronomy and Astrophysics Fellow.
Electronic address: jsokolos@cfa.harvard.edu

[1] See http://cxc.harvard.edu/ciao

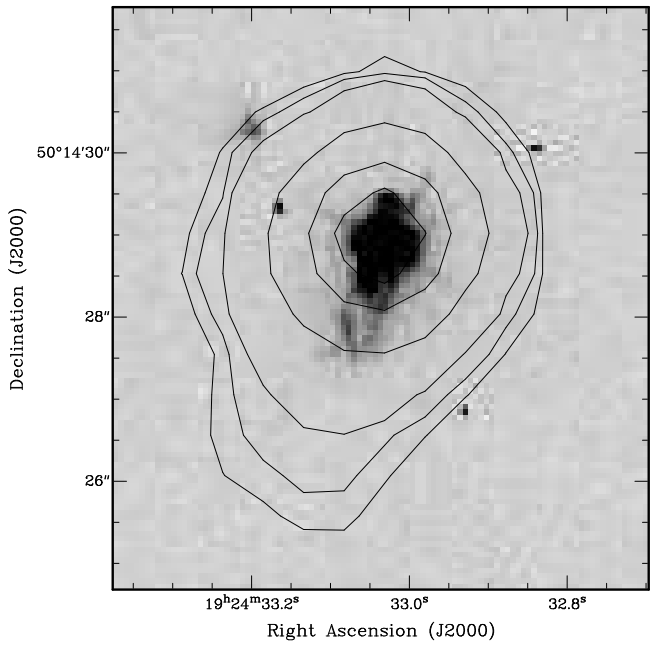

FIG. 1.— *Chandra* & *HST* images of the jet in CH Cyg. The contours show the zeroth order *Chandra* image from the 2001 March 27 observation, after smoothing with a Gaussian filter of radius 1". The contour values are 0.73, 1.2, 2, 10, 30, 50 and 90 counts per pixel. The greyscale shows the *HST* WFPC2 image from 1999 August 12 in the O III 495.9 nm & 500.7 nm filter (i.e. filter F502N); these data are also shown in Fig. 4c in Eyres et al. (2002).

which agrees to within 0.″11 with the *Hipparcos* position of the optical counterpart HD 182917 (Perryman et al. 1997). This offset is well within *Chandra*'s 90% pointing accuracy[2] of 0.″6. The binned zeroth order image of CH Cyg is shown in Fig. 1.

The source exhibited a faint extension $\sim$ 2–4″ to the south-southwest. At the source position, 38.″1 from the optical axis, no significant deviations from the optimal point-spread function (PSF) are expected (the 80% encircled energy radius for an on-axis point source is 0.″685 at $\approx$ 1 keV). For very bright sources, some fraction of the zeroth order photons can be spread out along the CCD columns passing close to the aimpoint (the "readout trace"), giving rise to spurious extensions to the zeroth-order image along that axis. However, at the count rate measured for CH Cyg, such effects are not significant. Furthermore, for the satellite roll angle during the observation, the readout axis was perpendicular to the observed extension. The position angle of the extended emission (measured anticlockwise through east from north) of the principal component of the photon distribution was 164°, consistent with contemporary measurements of the CH Cyg jet from VLA/MERLIN radio and HST optical measurements (Crocker et al. 2002). We therefore conclude that the extension observed in the *Chandra* image is due to X-ray emission from the jet in CH Cyg.

3.1. *Central Source*

We extracted a source spectrum using photons from within a circle of radius approximately 5″ around the centroid position. We used photons from an annulus 5–10″ from the centroid position as background. To improve the statistics for spectral fitting we binned the energy spectrum by a factor of 16. The spectrum exhibited two broad peaks, around 1 and 5 keV, as well as a prominent Fe Kα line (Fig. 2), as in previous observations (Wheatley 2001; Ezuka et al. 1998). After generating a response matrix and ancillary response file appropriate for the source position on the chip, we fitted the net spectrum with a model consisting of three Raymond-Smith (RS) plasma models and a Gaussian to describe the Fe Kα line (after Ezuka et al. 1998). We introduced neutral absorption multiplicative components with independent column densities for the two RS components with the highest temperatures, and a third absorption component applied to the entire model with the column density fixed at the value obtained from survey data, 7×10^{20} cm^{-2} (Stark et al. 1992). The softest RS component had $kT = 0.177\pm0.008$ keV (1σ error); for the other two components the fitted temperatures were 9.7 and 15 keV, but could only be constrained to be $\gtrsim$ 4 keV. The additional neutral absorption for the medium and hard RS components was $(5.0^{+1.8}_{-1.5})$ and $(58\pm9)\times10^{22}$ cm^{-2}, respectively. The (common) abundance for the RS components was $< 10^{-2}$ (3σ upper limit). The Fe Kα line energy was 6.62 ± 0.04 keV, with a FWHM of < 0.28 keV and an equivalent width of 480 eV. For this fit the C-statistic, which is the most appropriate statistic for low-count regimes, was 35.2, and 53% of 1000 Monte-Carlo spectral simulations gave a lower value, indicating a statistically acceptable fit.

We also fitted the zeroth order spectrum with a model consisting of emission from hot diffuse gas affected by an ionized absorber (following Wheatley 2001). The ionized column density exceeded the maximum of 10^{24} cm^{-2} allowed by the model; the 3σ lower limit for the column density was 8.6×10^{23} cm^{-2} (compared to 4×10^{23} from the *ASCA* spectrum; Wheatley 2001). The C-statistic was 104, and 100% of Monte-Carlo spectral simulations gave a lower value, indicating a poor fit. We therefore prefer the hot plasma model to the ionized absorber model.

By extrapolating our plasma model spectrum beyond the *Chandra* energy limits, we derive an intrinsic (unabsorbed) bolometric flux of 1.3×10^{-11} ergs cm^{-2} s^{-1}, giving a luminosity of 9.3×10^{31} ergs s^{-1} (for a distance of 245 pc). This luminosity is more than an order of magnitude smaller than typical values from earlier X-ray measurements of CH Cyg (e.g. Ezuka et al. 1998).

3.2. *X-Ray Jet*

We extracted 43 photons from the extended southern region, excluding photons within 1.″72 of the centroid position. The hardness ratio (calculated from the total counts > 2 keV divided by the counts < 2 keV), indicates that the extended emission (hardness ratio 0.65) was significantly softer than the central source (1.69). The photon distribution was however qualitatively similar to that of the zeroth-order image, with peaks below 1 keV and at 5 keV (Fig. 2). While this similarity suggests a similar spectral model for the jet, we detected an insufficient number of photons to exclude alternative models. To empirically characterize the jet spectrum, we fitted the data with an absorbed RS component for

[2] See http://cxc.harvard.edu/cal/ASPECT/celmon

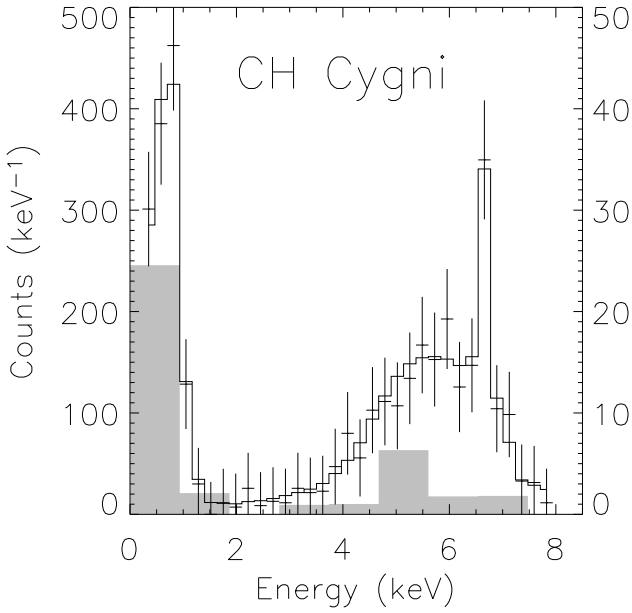

FIG. 2.— *Chandra* spectra from CH Cyg. The zeroth-order spectrum is shown as crosses, with error bars indicating the 1σ uncertainties. The dip in emission between 1–4 keV is not solely a consequence of a decreased effective area in that region. The histogram shows the best-fit model, consisting of 3 Raymond-Smith plasma components and a Gaussian to fit the line emission at 6.6 keV. The grey histgram shows the jet spectrum, scaled by a factor of 10 relative to the zeroth-order spectrum (right-hand y-axis).

the emission < 2 keV and a broad ($\sigma \approx 1$ keV) Gaussian for the emission > 2 keV, each affected by neutral absorption at the line-of-sight value of 7×10^{20} cm^{-2}. We found an acceptable fit (C-statistic of 4.0, below which fell only 6% of 1000 Monte-Carlo simulated spectra) with a plasma temperature of $0.18^{+0.06}_{-0.07}$ keV and a Gaussian center energy of $5.6^{+0.6}_{-0.5}$ keV. On extrapolating this model beyond the *Chandra* energy limits, we estimate a crude unabsorbed bolometric flux of 1.2×10^{-13} ergs cm^{-2} s^{-1}, giving a jet luminosity of 9×10^{29} ergs s^{-1}, or 1% of the source luminosity.

To further verify the source extension, we generated a simulated point-spread function (PSF) using the *Chandra* Ray-Tracer (ChaRT[3]) in combination with the Model of AXAF Response to X-rays (MARX[4]) simulation software. Using the fitted central-source spectral model as input to ChaRT, we simulated an observation of a point source at the observed position of CH Cyg, and generated an event file using MARX. We then measured the radial profile of the simulated zeroth-order image by extracting photons in a series of annulae at increasing diameters out to 10″ from the centroid position. The resulting point-spread function is shown as a grey ribbon in Fig. 3. We also measured the observed surface brightness profile of CH Cyg, both in the southern region where the source appeared extended, and over the rest of the image excluding this region. These two radial profiles are also plotted in Fig. 3. The extension we observed in the binned zeroth-order image of CH Cyg (Fig. 1) is apparent as an excess above the radial surface brightness profiles of both the simulated image and the non-southern directions of the observed images.

Using the same region from which we extracted the jet spectrum, we extracted only 4 photons from the simulated point-source image. We also expect 7 background photons, leading to a total of 11 photons expected from this region assuming a point-like source. Taking the photon counts within this region to be distributed according to Poisson statistics, the probability of observing 43 photons when 11 are expected is 1.67×10^{-13}, corresponding to a significance of 7.4σ. Thus, we confirm that the extension is genuine. We note that the northern optical jet is too small to be resolved with *Chandra*, and we see no evidence for extended emission in that direction.

4. DISCUSSION

4.1. *The X-ray Jet in CH Cygni*

The extended X-ray emission aligned with the optical and radio jets in CH Cyg can be naturally explained by the collision of a collimated outflow of material with surrounding nebular gas. Outflow velocities for CH Cyg have been estimated from at least two of the four recorded jet ejections: 600–2000 km s^{-1} and 1100 km s^{-1} in 1984/1985 (Taylor et al. 1986 and references therein, and Crocker et al. 2001 respectively), and > 1100 km s^{-1} in 1998-2000 (Eyres et al. 2002) For a typical outflow velocity of ~ 1300 km s^{-1}, the Rankine-Hugoniot jump conditions give $v_s = (4/3)v_{\rm flow} \approx 1700$ km s^{-1} (where v_s is the shock velocity and $v_{\rm flow}$ is the flow speed in the jet) for a strong shock. The temperature behind the shock, $T_{\rm ps}$, is

$$T_{\rm ps} = \frac{3}{16}\frac{\mu m_p}{k_B} v_s^2 = 4 \times 10^7 \left(\frac{v_s}{1700\ {\rm km\,s^{-1}}}\right)^2 \left(\frac{\mu}{0.6}\right)\ {\rm K}, \quad (1)$$

where μ is the mean molecular weight, k_B is Boltzmann's

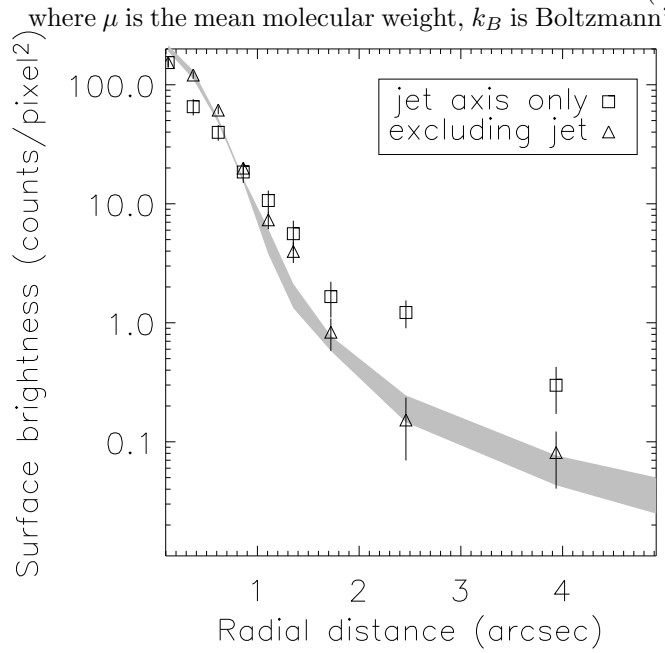

FIG. 3.— Radial surface brightness profiles of the zeroth-order *Chandra* image of CH Cyg. The grey ribbon shows the $\pm 1\sigma$ limits on the simulated PSF from ChaRT/MARX, while the triangles show the radial profiles calculated using annulae excluding the southern extension. The squares show the radial profile for the southern extension. Error bars indicate the 1σ uncertainties.

[3] See http://cxc.harvard.edu/chart
[4] See http://space.mit.edu/CXC/MARX

constant, m_P is the proton mass, and we have assumed that the gas is ideal. Even if the shock is collisionless, the electrons behind the shock attain temperature equilibrium with the ions in just a few months (Spitzer 1978). A plasma with a post-shock temperature of 4×10^7 K produces X-rays in the 4-5 keV range; although we have insufficient jet X-ray photons to perform formal spectral fitting, we detect X-ray-jet photons at these energies. The data are thus consistent with material heated in a strong shock.

Softer X-ray photons are also detected from the jet. Although the cooling time for optically thin thermal Bremsstrahlung emission is much longer than the age of the jet, the time scale for hot plasma to cool by flowing out to the sides of the jet from behind the shock is given roughly by the width of the jet divided by the sound speed. For the jet parameters of CH Cyg, this time is approximately a few months. Thus, if adiabatic expansion plays a significant role in cooling the post-shock plasma, the lower-temperature jet emission (photons around 1 keV) could be due to material that has expanded perpendicular to the flow of the jet, and cooled.

Adopting $v_s = 1700\mathrm{km, s^{-1}}$ and a jet size of $4''$ on 2001 March 27, we can estimate the epoch of jet production. For $d = 245$ pc, we derive a mean proper motion for the jet of $1\farcs46$ yr^{-1}. The extended *Chandra* emission is therefore consistent with having been produced by material that was ejected in mid-1998. At that time, CH Cyg underwent a transition into an optical high state (see e.g. Crocker et al. 2001; Eyres et al. 2002; Sokoloski & Kenyon 2003b). The detection of extended radio emission in 1995 by Crocker et al. (2001) suggests that a jet ejection also occurred in association with a transition to the optical high state in 1992. The other two jet ejections, in 1984/85 (Taylor et al. 1986) and 1997 (Karovska et al. 1998), were associated instead with transitions from optical high to optical low states. Thus there are at least two different scenarios in which jets can be produced in CH Cyg. This situation is reminiscent of X-ray binaries, which can produce discrete ejections in association with X-ray state changes, possibly in response to an extreme physical change in the accretion flow (Fender & Hendry 2000).

4.2. *Non-relativistic X-ray Jets*

The only other symbiotic star currently known to have an X-ray jet, is R Aqr (see Kellogg et al. 2001). Compared to CH Cyg the R Aqr jet is both more extended on the sky ($30''$ for the R Aqr southern jet compared to $4''$ for CH Cyg) and physically larger (roughly 6000 AU compared to roughly 1000 AU for CH Cyg). Although the measured jet fluxes for the two sources are comparable, Kellogg et al. (2001) found that few of the jet X-ray photons from R Aqr had energies greater than 1 keV. The R Aqr jet spectrum revealed emission lines at 400 and 550 eV and was generally consistent with a shocked plasma out of ionization equilibrium (the plasma temperatures for the northeastern and southwestern jets were found to be 2×10^7 K and 2×10^6 K respectively). A follow-up *Chandra* observation of R Aqr revealed that

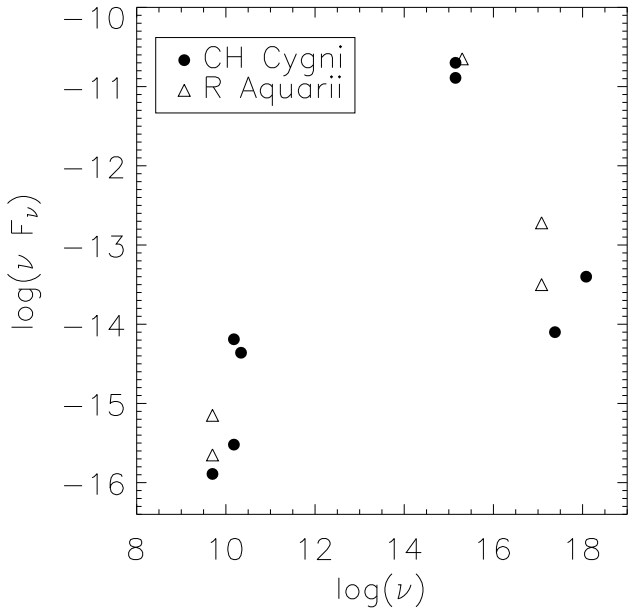

Fig. 4.— Comparison of the spectral energy distributions for the jet emission from CH Cyg (filled circles) and R Aqr (open triangles). The radio data for CH Cyg are from Crocker et al. (2001) and Karovska et al. (1998), and for R Aqr are from Dougherty et al. (1995), Lehto & Johnson (1992) and Kafatos et al. (1989). The UV data for CH Cyg are from Eyres et al. (2002), and for R Aqr are from Contini & Formiggini (2003). The X-ray measurements for CH Cyg are from this paper, and for R Aqr are from Kellogg et al. (2001). There is significant uncertainty on each individual point because both the CH Cyg and R Aqr jets are variable. Also, the UV fluxes for CH Cyg are not extinction corrected, and it is not known whether the UV flux for R Aqr from Contini & Formiggini (2003) is extinction corrected (CH Cyg and R Aqr are at similar distances, and both out of the plane of the Galaxy). Finally, the CH Cyg jet X-ray fluxes are absorption corrected using the Galactic column only, and the local absorption might be much larger.

the northern R Aqr X-ray jet is expanding at a velocity of approximately 600 km s^{-1} (E. Kellogg, private communication). Contini & Formiggini (2003) compiled and modeled the full spectral energy distribution (SED) of R Aqr, and found that the jet emission is due to a combination of photoionization and shock heating. In units of νF_ν, where ν is radiation frequency and F_ν is flux density, the R Aqr jet emission is strongest in the UV, weakest in the radio, and somewhere in between for the X-rays. In Fig. 4 we plot both the SED data compiled for R Aqr by Contini & Formiggini (2003) and that for CH Cyg obtained from the literature and our work in the X-rays. The jet SEDs for R Aqr and CH Cyg are quite similar, despite some differences in jet properties (R Aqr appears to have a slower shock speed, slightly lower post-shock temperatures, and a larger size). This similarity suggests that other symbiotic-star jets might also be expected to emit X-rays.

In addition to symbiotic-star jets, two other types of non-relativistic jet have been detected in the X-rays: protostellar jets (in Herbig-Haro objects) and collimated outflows from the central stars or binaries in planetary nebulae (PNe). In both cases, the X-rays also appear to be due to shock heating as the outflowing material collides with surrounding gas. The first X-ray bright protostellar outflow, in HH2, was discovered by Pravdo et al.

(2001). Shortly afterwards, X-ray emission was reported from the protostellar jet L1551 IRS5 (HH 154) by Favata et al. (2002). In both systems, the protostellar-jet X-ray luminosities are a few times 10^{29} ergs (similar to CH Cyg and R Aqr) and the jet plasma temperatures are $\sim 10^6$ K. Soker & Kastner (2003) summarize six observations of PNe by *Chandra* and *XMM*, four of which revealed diffuse X-ray emission with temperatures of a few time 10^6 K. These four PNe all show evidence for high-velocity, collimated flows (Kastner et al. 2003). Soker & Kastner (2003) suggest that a hidden binary companion within each of these PNe accrete from the AGB-star wind and produce an X-ray jet. They note that the X-ray production mechanism would thus be similar to that in the protostellar outflows mentioned above, and the symbiotic star R Aqr. In fact, an additional PNe with X-ray-jet emission, Menzel 3, is known to contain a symbiotic pair at its center (Kastner et al. 2003; Zhang & Liu 2002; Schmeja & Kimeswenger 2001). The links between the X-ray jets in symbiotic stars, protostellar outflows, and PNe are thus quite compelling.

We thank J. Lazendic for help generating and overlaying the images. We are also grateful to J. Raymond and S. Kenyon for useful discussion. This work was funded in part by the NASA Long Term Space Astrophysics program under grant NAG 5-9184 (PI: Chakrabarty). JLS is supported by an NSF Astronomy and Astrophysics Postdoctoral Fellowship under award AST-0302055. This research has made use of data obtained through the High Energy Astrophysics Science Archive Research Center Online Service, provided by the NASA/Goddard Space Flight Center.

REFERENCES

Brocksopp, C., Sokoloski, J. L., Kaiser, C., Richards, A. M., Muxlow, T. W. B., & Seymour, N. 2004, MNRAS, 347, 430
Contini, M. & Formiggini, L. 2003, MNRAS, 339, 148
Corradi, R. L. M., Munari, U., Livio, M., Mampaso, A., Gonçalves, D. R., & Schwarz, H. E. 2001, ApJ, 560, 912
Crocker, M. M., Davis, R. J., Eyres, S. P. S., Bode, M. F., Taylor, A. R., Skopal, A., & Kenny, H. T. 2001, MNRAS, 326, 781
Crocker, M. M., Davis, R. J., Spencer, R. E., Eyres, S. P. S., Bode, M. F., & Skopal, A. 2002, MNRAS, 335, 1100
Dougherty, S. M., Bode, M. F., Lloyd, H. M., Davis, R. J., & Eyres, S. P. 1995, MNRAS, 272, 843
Eyres, S. P. S., Bode, M. F., Skopal, A., Crocker, M. M., Davis, R. J., Taylor, A. R., Teodorani, M., Errico, L., Vittone, A. A., & Elkin, V. G. 2002, MNRAS, 335, 526
Ezuka, H., Ishida, M., & Makino, F. 1998, ApJ, 499, 388
Favata, F., Fridlund, C. V. M., Micela, G., Sciortino, S., & Kaas, A. A. 2002, A&A, 386, 204
Fender, R. & Hendry, M. 2000, MNRAS, 317 (1), 1
Hinkle, K. H., Fekel, F. C., Johnson, D. S., & Scharlach, W. W. G. 1993, AJ, 105, 1074
Ivison, R. J., Bode, M. F., Roberts, J. A., Meaburn, J., Davis, R. J., Nelson, R. F., & Spencer, R. E. 1991, MNRAS, 249, 374
Kafatos, M., Hollis, J. M., Yusef-Zadeh, F., Michalitsianos, A. G., & Elitzur, M. 1989, ApJ, 346, 991
Karovska, M., Carilli, C. L., & Mattei, J. A. 1998, Journal of the American Association of Variable Star Observers (JAAVSO), 26, 97
Kastner, J. H., Balick, B., Blackman, E. G., Frank, A., Soker, N., Vrtílek, S. D., & Li, J. 2003, ApJ, 591, L37
Kellogg, E., Pedelty, J. A., & Lyon, R. G. 2001, ApJ, 563, L151
Kenyon, S. J. 1986, The symbiotic stars (Cambridge and New York: Cambridge University Press), 295
—. 2001, in Encyclopedia of Astronomy and Astrophysics, ed. P. Murdin (London: Institute of Physics)
Leahy, D. A. & Taylor, A. R. 1987, A&A, 176, 262
Lehto, H. J. & Johnson, D. R. H. 1992, Nature, 355, 705
Munari, U., Yudin, B. F., Kolotilov, E. A., & Tomov, T. V. 1996, A&A, 311, 484
Perryman, M. A. C., Lindegren, L., Kovalevsky, J., Hoeg, E., Bastian, U., Bernacca, P. L., Crézé, M., Donati, F., Grenon, M., van Leeuwen, F., van der Marel, H., Mignard, F., Murray, C. A., Le Poole, R. S., Schrijver, H., Turon, C., Arenou, F., Froeschlé, M., & Petersen, C. S. 1997, A&A, 323, L49
Pravdo, S. H., Feigelson, E. D., Garmire, G., Maeda, Y., Tsuboi, Y., & Bally, J. 2001, Nature, 413, 708
Schmeja, S. & Kimeswenger, S. 2001, A&A, 377, L18
Soker, N. & Kastner, J. H. 2003, ApJ, 583, 368
Sokoloski, J. L. & Kenyon, S. J. 2003a, ApJ, 584, 1021
—. 2003b, ApJ, 584, 1027
Spitzer, L. 1978, Physical processes in the interstellar medium (New York: Wiley-Interscience), 333
Stark, A. A., Gammie, C. F., Wilson, R. W., Bally, J., Linke, R. A., Heiles, C., & Hurwitz, M. 1992, ApJS, 79, 77
Taylor, A. R., Seaquist, E. R., & Mattei, J. A. 1986, Nature, 319, 38
Viotti, R., Badiali, M., Cardini, D., Emanuele, A., & Iijima, T. 1997, in ESA SP-402: Hipparcos - Venice '97, 405–408
Weisskopf, M. C., Brinkman, B., Canizares, C., Garmire, G., Murray, S., & Van Speybroeck, L. P. 2002, PASP, 114, 1
Wheatley, P. J. 2001, in AIP Conf. Proc. 599: X-ray Astronomy: Stellar Endpoints, AGN, and the Diffuse X-ray Background, 1007–1010
Zhang, Y. & Liu, X.-W. 2002, MNRAS, 337, 499